Pergamon

Int. J. Solids Structures Vol. 31, No. 4, pp. 567–586, 1994

0020–7683/94 $6.00 + .00

THE ELASTIC FIELD FOR AN UPRIGHT OR TILTED SLIDING CIRCULAR FLAT PUNCH ON A TRANSVERSELY ISOTROPIC HALF SPACE

M. T. HANSON
Department of Engineering Mechanics, University of Kentucky,
Lexington, Kentucky 40506-0046, U.S.A.

(*Received* 5 *June* 1992; *in revised form* 26 *July* 1993)

Abstract—This paper gives closed form expressions for the displacement and stress fields in a transversely isotropic half space when the surface is loaded in shear by a sliding circular flat punch in either an upright or inclined position. The shear traction on the surface is taken as a friction coefficient multiplied by the frictionless contact pressure. The solution derived here for shear loading is generally approximate since the interaction between the normal and shear loading is ignored and the relative displacements do not necessarily align to the direction of shear traction. However, it is shown that the interaction between the surface stresses vanishes for a particular value of the elastic constants and it is also shown that in some instances the tangential displacements do align with the shear traction thus yielding an exact solution. It is furthermore shown that the solution for a sliding flat upright indenter is an exact solution to the problem of a circular external crack in an infinite transversely isotropic body subjected to uniform tangential displacement loading at infinity. Numerical results for the subsurface stress fields are given to illustrate the effects of sliding and transverse isotropy.

1. INTRODUCTION

Problems concerning the contact between elastic bodies have been of great interest to researchers over the past century. As a special case, the class of three-dimensional rigid punch problems in contact with an elastic half space have been the topic of a considerable number of investigations. A good review of this literature can be found in Gladwell (1980). Although the list of references on this subject is extensive, most of this previous work has dealt with calculating quantities on the surface only and most have considered only isotropic materials. Very few investigators have evaluated closed form expressions for the elastic field and even less have considered transversely isotropic materials. The indenter geometry may take many different forms but attention here is focused on the problem of a rigid right circular cylinder pressed into a transversely isotropic elastic half space in either an upright or inclined position. The other classic cases of conical and spherical (Hertzian) indentation have been considered previously by the author (Hanson 1992a, b, 1993a, b) and will not be discussed presently.

Sneddon (1946) was the first investigator to give explicit expressions for the elastic field resulting from frictionless indentation of an isotropic half space by a flat ended circular cylinder. Muki (1960) considered the nonaxisymmetric case when the indenter is acted upon by moments, again for isotropy. Apparently Elliot (1949) was the first to give the elastic field resulting from frictionless indentation of a transversely isotropic half space by a rigid right circular cylinder in an upright position. The displacements and stresses were given in terms of inverse Hankel transform integrals which he noted could be evaluated by methods given in Watson (1980). Very recently, Fabrikant (1988) has given explicit closed form expressions for the elastic field for this problem. In addition, he also gave the elastic field for the nonaxisymmetric case when the indenter is acted upon by moments and the net normal force is zero. The elastic field for a circular flat indenter under nonconcentric normal loading can be simply obtained by superposing these two separate solutions.

All previous analysis has considered the frictionless case only. In some circumstances the indenter may also be subjected to tangential loading thus possibly causing the indenter to slide on the surface. Shear loading of three-dimensional indenters is a very difficult problem and has not been addressed previously in the literature except for the well known Hertzian contact analysis and the conical indentation solution noted earlier. The present

study is an attempt to consider this possible loading condition for both the flat and the tilted indenter. It is assumed in this analysis that the indenter slides across the surface and a Coulomb friction law is used. The shear traction is thus taken as a coefficient of friction multiplied by the contact pressure. It is important to note two key factors which render this solution approximate. First, the effect of shear loading will alter the surface profile and hence the contact pressure will differ to some extent from the frictionless pressure distribution used here. Secondly, the shear stress will not align to oppose relative motion. This results in points on the contact surface having tangential displacements in two directions when the shear traction is only unidirectional. It is important to point out that no exact closed form solution for tangential loading of rigid indentation of an elastic half space has ever been presented in the literature. The present solution, although containing approximations, is the first closed form solution to this problem for right circular cylindrical indentation.

It will be shown that for the sliding upright indenter, the tangential displacements are constant inside the loaded region and always align with the direction of shear traction for any transversely isotropic material. This was shown to be true previously by Mindlin (1949) for isotropy and Fabrikant (1989) for transverse isotropy. Furthermore, for a particular value of the elastic constants (when the parameter $\alpha = 0$) the shear traction will not affect the contact pressure. In this case the presently derived solution is an exact one. For the sliding tilted indenter, the tangential displacements do not generally align with the shear traction unless a relation between the elastic constants is zero ($G_2 = 0$ where G_2 is a parameter). As with the upright indenter, the shear loading will not affect the contact pressure if $\alpha = 0$. If these two relations are satisfied the present solution for the tilted indenter is again exact under sliding conditions.

One of the solutions derived here is also pertinent to the area of fracture mechanics. It will be shown that for the flat upright indenter, the tangential sliding traction on the surface produces a tangential surface displacement which is constant inside the loaded region. Since all traction vanishes outside the circular contact area, this problem is shown to be equivalent to a circular external crack in an infinite transversely isotropic body loaded by a uniform remote tangential displacement parallel to the crack plane. The present results provide the elastic field in closed form for this problem. The closed form solution to this problem for isotropy has been given by Westmann (1965).

2. POTENTIAL FUNCTIONS AND GREEN'S FUNCTIONS FOR TRANSVERSE ISOTROPY

Consider a transversely isotropic elastic half space $z > 0$ where the surface $z = 0$ is parallel to the plane of isotropy, Fig. 1. The notation of Fabrikant (1988, 1989) will be adopted. The displacements are denoted as u, v and w in the x, y and z directions and A_{11}, A_{13}, A_{33}, A_{44} and A_{66} are the five elastic constants. The relations giving the displacements

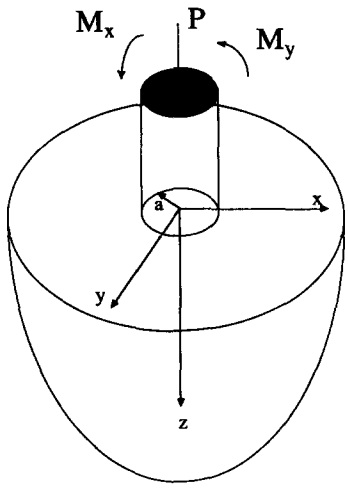

Fig. 1. Geometry and coordinate system for indentation.

and stresses in terms of the three potentials F_1, F_2 and F_3 can be found in the above references. Following previous research, the complex displacement $u^c = u+iv$ will be used along with the stress combinations $\sigma_1 = \sigma_{xx}+\sigma_{yy}$, $\sigma_2 = \sigma_{xx}-\sigma_{yy}+2i\tau_{xy}$ and $\tau_z = \tau_{xz}+i\tau_{yz}$.

To obtain the solution for a distributed loading, integration of the point force solutions will be used. For this purpose cylindrical coordinates ρ, ϕ, z are adopted. The point force is applied on the surface $z = 0$ at the point ρ_o, ϕ_o with components T_x, T_y in the positive x and y directions, respectively.

The potential functions for the point shear loading are given as (see Fabrikant, 1989; Hanson, 1992a, b)

$$F_1(\rho,\phi,z;\rho_o,\phi_o) = \frac{H\gamma_1}{(m_1-1)}\frac{\gamma_2}{2}(T\bar{\Lambda}+\bar{T}\Lambda)\chi(z_1), \tag{1}$$

$$F_2(\rho,\phi,z;\rho_o,\phi_o) = \frac{H\gamma_2}{(m_2-1)}\frac{\gamma_1}{2}(T\bar{\Lambda}+\bar{T}\Lambda)\chi(z_2), \tag{2}$$

$$F_3(\rho,\phi,z;\rho_o,\phi_o) = i\frac{\gamma_3}{4\pi A_{44}}(T\bar{\Lambda}-\bar{T}\Lambda)\chi(z_3), \tag{3}$$

where $T = T_x+iT_y$, an overbar indicates complex conjugation, the function $\chi(z_k)$ is:

$$\chi(z_k) = (z_k \ln[R_k+z_k]-R_k), \quad k = 1,2,3, \tag{4}$$

and

$$R_k^2 = \rho^2+\rho_o^2-2\rho\rho_o\cos(\phi-\phi_o)+z_k^2, \quad z_k = \frac{z}{\gamma_k}, \quad k = 1,2,3. \tag{5}$$

The constant H is defined as:

$$H = \frac{(\gamma_1+\gamma_2)A_{11}}{2\pi(A_{11}A_{33}-A_{13}^2)}. \tag{6}$$

3. ELASTIC FIELD FOR SLIDING FLAT INDENTATION

The problem under consideration is shown in Fig. 1. A circular flat indenter is pressed into an elastic half space by a force P and the moments M_x and M_y are zero. The indenter displacement is denoted as ω and the contact circle has a radius of $\rho = a$. The elastic field is obtained by first evaluating the potential functions and then differentiating. The potential function and the elastic field for frictionless indentation has been given by Fabrikant (1988). He derived the relationship between the indenter force P and indentation depth ω as $P\pi H = 2a\omega$. Here sliding of the indenter is considered and a Coulomb friction law is used. The shear traction is taken as a friction coefficient multiplied by the frictionless contact pressure. Since only shear traction is considered presently, the solution for frictionless indentation given by Fabrikant (1988) must be added to the results here to obtain the complete solution for indentation and sliding.

The potential functions for shear loading can be obtained by integrating the point force solutions above. The frictionless contact pressure is identical to the isotropic case and it is given as

$$\sigma_{zz}(\rho,\phi,0) = -\frac{P}{2\pi a}\frac{1}{\sqrt{a^2-\rho^2}}, \quad 0 < \rho < a.$$

Using f_x and f_y as the coefficients of friction in the x and y directions, the complex shear force $T = T_x+iT_y$ in the potential functions of equations (1)–(3) is replaced as:

$$T = \frac{fP}{2\pi a}\frac{1}{\sqrt{a^2-\rho_o^2}}\rho_o\,\mathrm{d}\rho_o\,\mathrm{d}\phi_o, \quad f = f_x + if_y, \tag{7}$$

and the result is integrated on $0 < \rho_o < a$, $0 < \phi_o < 2\pi$. The potentials become:

$$F_1(\rho,\phi,z) = \frac{H\gamma_1\gamma_2}{(m_1-1)}\frac{P}{4\pi a}(f\bar{\Lambda}+\bar{f}\Lambda)[z_1\psi(\rho,\phi,z_1)-\Phi(\rho,\phi,z_1)], \tag{8}$$

$$F_2(\rho,\phi,z) = \frac{H\gamma_1\gamma_2}{(m_2-1)}\frac{P}{4\pi a}(f\bar{\Lambda}+\bar{f}\Lambda)[z_2\psi(\rho,\phi,z_2)-\Phi(\rho,\phi,z_2)], \tag{9}$$

$$F_3(\rho,\phi,z) = i\frac{P\gamma_3}{8\pi^2 a A_{44}}(f\bar{\Lambda}-\bar{f}\Lambda)[z_3\psi(\rho,\phi,z_3)-\Phi(\rho,\phi,z_3)], \tag{10}$$

where

$$\psi(\rho,\phi,z) = \int_0^{2\pi}\int_0^a \frac{1}{\sqrt{a^2-\rho_o^2}}\ln[R+z]\rho_o\,\mathrm{d}\rho_o\,\mathrm{d}\phi_o, \tag{11}$$

$$\Phi(\rho,\phi,z) = \int_0^{2\pi}\int_0^a \frac{1}{\sqrt{a^2-\rho_o^2}}R\rho_o\,\mathrm{d}\rho_o\,\mathrm{d}\phi_o, \tag{12}$$

and $R^2 = \rho^2+\rho_o^2-2\rho\rho_o\cos(\phi-\phi_o)+z^2$.

The potential function $\psi(\rho,\phi,z)$ corresponds to frictionless indentation and it was evaluated by Fabrikant (1988) as:

$$\psi(\rho,\phi,z) = 2\pi\left((z)\sin^{-1}\frac{\ell_1(a)}{\rho}+a\ln[\ell_2(a)+\sqrt{\ell_2^2(a)-\rho^2}]-\sqrt{a^2-\ell_1^2(a)}\right). \tag{13}$$

The potential function $\Phi(\rho,\phi,z)$ is evaluated in Appendix B as:

$$\Phi(\rho,\phi,z) = \frac{\pi}{2}\left\{(2a^2+2z^2+\rho^2)\sin^{-1}\frac{\ell_1(a)}{\rho}+\frac{1}{a}(2a^2+\ell_1^2(a))\sqrt{\ell_2^2(a)-a^2}\right\}. \tag{14}$$

The quantities $\ell_1(a)$ and $\ell_2(a)$ are defined as:

$$\begin{aligned}\ell_1(a) &= \tfrac{1}{2}(\sqrt{(\rho+a)^2+z^2}-\sqrt{(\rho-a)^2+z^2}),\\ \ell_2(a) &= \tfrac{1}{2}(\sqrt{(\rho+a)^2+z^2}+\sqrt{(\rho-a)^2+z^2}).\end{aligned} \tag{15}$$

The elastic field resulting from the shear traction can be evaluated by performing appropriate differentiations of the potential functions above. The differentiations of $\psi(\rho,\phi,z)$ are tabulated in Appendix A and those for $\Phi(\rho,\phi,z)$ are given in Appendix B. The elastic field is:

$$\begin{aligned}u^e = \frac{HP}{2a}\gamma_1\gamma_2\sum_{k=1}^{2}\frac{1}{(m_k-1)}\Bigg[&-f\sin^{-1}\frac{\ell_{1k}(a)}{\rho}+\bar{f}\,\mathrm{e}^{i2\phi}\left\{\frac{2z_k}{\rho^2}\sqrt{a^2-\ell_{1k}^2(a)}\right.\\ &\left.-\frac{2az_k}{\rho^2}+\frac{\ell_{1k}(a)}{\rho^2}\sqrt{\rho^2-\ell_{1k}^2(a)}\right\}\Bigg]+\frac{P\gamma_3}{4\pi a A_{44}}\Bigg[f\sin^{-1}\frac{\ell_{13}(a)}{\rho}+\bar{f}\,\mathrm{e}^{i2\phi}\left\{\frac{2z_3}{\rho^2}\sqrt{a^2-\ell_{13}^2(a)}\right.\\ &\left.-\frac{2az_3}{\rho^2}+\frac{\ell_{13}(a)}{\rho^2}\sqrt{\rho^2-\ell_{13}^2(a)}\right\}\Bigg],\end{aligned} \tag{16}$$

$$w = \frac{HP\gamma_1\gamma_2}{2a}(\bar{f}\,e^{i\phi}+f\,e^{-i\phi})\sum_{k=1}^{2}\frac{m_k}{(m_k-1)\gamma_k}\left\{\frac{a}{\rho}-\frac{\sqrt{a^2-\ell_{1k}^2(a)}}{\rho}\right\}, \tag{17}$$

$$\sigma_1 = -\frac{HPA_{66}\gamma_1\gamma_2}{a}(\bar{f}\,e^{i\phi}+f\,e^{-i\phi})\sum_{k=1}^{2}\frac{[\gamma_k^2-(1+m_k)\gamma_3^2]}{\gamma_k^2(m_k-1)}\frac{\ell_{1k}(a)\sqrt{\rho^2-\ell_{1k}^2(a)}}{\rho[\ell_{2k}^2(a)-\ell_{1k}^2(a)]}, \tag{18}$$

$$\begin{aligned}\sigma_2 = \frac{HPA_{66}\gamma_1\gamma_2}{a}\sum_{k=1}^{2}\frac{1}{(m_k-1)}\Bigg[&f\,e^{i\phi}\frac{\ell_{1k}(a)\sqrt{\rho^2-\ell_{1k}^2(a)}}{\rho[\ell_{2k}^2(a)-\ell_{1k}^2(a)]}\\&+\bar{f}\,e^{i3\phi}\left\{\frac{8az_k}{\rho^3}-\frac{\sqrt{\rho^2-\ell_{1k}^2(a)}}{\rho^3\ell_{1k}(a)[\ell_{2k}^2(a)-\ell_{1k}^2(a)]}(8a^2\ell_{2k}^2(a)-8a^2\rho^2\right.\\&\left.+(3\rho^2-4a^2+4z_k^2)\ell_{1k}^2(a))\right\}\Bigg]-\frac{P}{2\pi a\gamma_3}\Bigg[f\,e^{i\phi}\frac{\ell_{13}(a)\sqrt{\rho^2-\ell_{13}^2(a)}}{\rho[\ell_{23}^2(a)-\ell_{13}^2(a)]}\\&-\bar{f}\,e^{i3\phi}\left\{\frac{8az_3}{\rho^3}-\frac{\sqrt{\rho^2-\ell_{13}^2(a)}}{\rho^3 l_{13}(a)[\ell_{23}^2(a)-\ell_{13}^2(a)]}(8a^2\ell_{23}^2(a)-8a^2\rho^2\right.\\&\left.+(3\rho^2-4a^2+4z_3^2)\ell_{13}^2(a))\right\}\Bigg],\end{aligned} \tag{19}$$

$$\sigma_{zz} = \frac{P\gamma_1\gamma_2}{4\pi a(\gamma_1-\gamma_2)}(\bar{f}\,e^{i\phi}+f\,e^{-i\phi})\sum_{k=1}^{2}(-1)^k\frac{\ell_{1k}(a)\sqrt{\rho^2-\ell_{1k}^2(a)}}{\rho[\ell_{2k}^2(a)-\ell_{1k}^2(a)]}, \tag{20}$$

$$\begin{aligned}\tau_z = \frac{P\gamma_1\gamma_2}{4\pi a(\gamma_1-\gamma_2)}\sum_{k=1}^{2}\frac{(-1)^{k+1}}{\gamma_k}\Bigg[&f\frac{\sqrt{a^2-\ell_{1k}^2(a)}}{[\ell_{2k}^2(a)-\ell_{1k}^2(a)]}\\&+\bar{f}\,e^{i2\phi}\left\{\frac{\sqrt{a^2-\ell_{1k}^2(a)}}{[\ell_{2k}^2(a)-\ell_{1k}^2(a)]}-\frac{2a}{\rho^2}+\frac{2}{\rho^2}\sqrt{a^2-\ell_{1k}^2(a)}\right\}\Bigg]\\-\frac{P}{4\pi a}\Bigg[&f\frac{\sqrt{a^2-\ell_{13}^2(a)}}{[\ell_{23}^2(a)-\ell_{13}^2(a)]}-\bar{f}\,e^{i2\phi}\left\{\frac{\sqrt{a^2-\ell_{13}^2(a)}}{[\ell_{23}^2(a)-\ell_{13}^2(a)]}-\frac{2a}{\rho^2}+\frac{2}{\rho^2}\sqrt{a^2-\ell_{13}^2(a)}\right\}\Bigg],\end{aligned} \tag{21}$$

where the notation

$$\ell_{1k}^2(a) = \tfrac{1}{2}(\sqrt{(\rho+a)^2+z_k^2}-\sqrt{(\rho-a)^2+z_k^2}), \tag{22}$$

has been introduced along with a similar interpretation for $\ell_{2k}(a)$.

4. ELASTIC FIELD FOR A SLIDING TILTED INDENTER

Now consider the indentation problem shown in Fig. 1 where the circular flat indenter is acted upon by moments M_x and M_y about the x- and y-axis, respectively and the net force on the indenter is zero. The rotations of the indenter about the x- and y-axis are b_x and b_y. The potential function and the elastic field for frictionless indentation is given by Fabrikant (1988). He derived the relation between the complex moment $M = M_x+iM_y$ and rotation $b = b_x+ib_y$ as $M = (4a^3/3\pi H)b$.

Sliding of the indenter is now considered with the shear stress in the contact region taken as a friction coefficient multiplied by the frictionless contact pressure. Again the solution for shear loading only is given below and the complete solution requires superposing the elastic field for frictionless indentation. The frictionless contact pressure is identical to the isotropic case and is given as

$$\sigma_{zz}(\rho,\phi,0) = -\frac{3}{2\pi a^3}\frac{M_x\rho\sin\phi - M_y\rho\cos\phi}{\sqrt{a^2-\rho^2}}, \quad 0<\rho<a.$$

Proceeding in a manner identical to the previous case the potentials are now:

$$F_1(\rho,\phi,z) = \frac{3H\gamma_1\gamma_2}{(m_1-1)}\frac{1}{4\pi a^3}(f\bar{\Lambda}+\bar{f}\Lambda)(z_1\psi(\rho,\phi,z_1)-\Phi(\rho,\phi,z_1)), \tag{23}$$

$$F_2(\rho,\phi,z) = \frac{3H\gamma_1\gamma_2}{(m_2-1)}\frac{1}{4\pi a^3}(f\bar{\Lambda}+\bar{f}\Lambda)(z_2\psi(\rho,\phi,z_2)-\Phi(\rho,\phi,z_2)), \tag{24}$$

$$F_3(\rho,\phi,z) = i\frac{3\gamma_3}{8\pi^2 a^3 A_{44}}(f\bar{\Lambda}-\bar{f}\Lambda)(z_3\psi(\rho,\phi,z_3)-\Phi(\rho,\phi,z_3)), \tag{25}$$

with

$$\psi(\rho,\phi,z) = Im\left\{\bar{M}\int_0^{2\pi}\int_0^a \frac{\rho_o\,e^{i\phi_o}}{\sqrt{a^2-\rho_o^2}}\ln[R+z]\rho_o\,d\rho_o\,d\phi_o\right\}, \tag{26}$$

$$\Phi(\rho,\phi,z) = Im\left\{\bar{M}\int_0^{2\pi}\int_0^a \frac{\rho_o\,e^{i\phi_o}}{\sqrt{a^2-\rho_o^2}}R\rho_o\,d\rho_o\,d\phi_o\right\}, \tag{27}$$

where *Im* stands for the imaginary part. The potential function $\psi(\rho,\phi,z)$ is for frictionless indentation and can be extracted from Fabrikant (1988) as

$$\psi(\rho,\phi,z) = \frac{\pi i}{2}(M\rho\,e^{-i\phi}-\bar{M}\rho\,e^{i\phi})\left\{z\sin^{-1}\frac{\ell_1(a)}{\rho}-\frac{2a^3}{3\rho^2}\right.$$
$$\left.-\sqrt{a^2-\ell_1^2(a)}\left(1-\frac{2a^2+\ell_1^2(a)}{3\rho^2}\right)\right\}. \tag{28}$$

The potential function $\Phi(\rho,\phi,z)$ is evaluated in Appendix D as:

$$\Phi(\rho,\phi,z) = \frac{\pi i}{2}(M\rho\,e^{-i\phi}-\bar{M}\rho\,e^{i\phi})\left\{\tfrac{1}{8}(\rho^2+4z^2-4a^2)\sin^{-1}\frac{\ell_1(a)}{\rho}\right.$$
$$\left.-(\ell_1^2(a)+2\ell_2^2(a)-\tfrac{3}{2}\rho^2)\frac{\ell_1(a)\sqrt{\rho^2-\ell_1^2(a)}}{4\rho^2}\right\}. \tag{29}$$

The elastic field for shear loading is found by differentiation of the potentials. The derivatives are given in Appendix C for $\psi(\rho,\phi,z)$ and Appendix D for $\Phi(\rho,\phi,z)$. The elastic field can be written as:

$$u^c = \frac{3Hi}{8a^3}\gamma_1\gamma_2\sum_{k=1}^{2}\frac{1}{(m_k-1)}\left[(f\bar{M}\,e^{i\phi}-fM\,e^{-i\phi}-\bar{f}M\,e^{i\phi})\left(\rho\sin^{-1}\frac{\ell_{1k}(a)}{\rho}\right.\right.$$
$$\left.-\frac{1}{\rho}\ell_{1k}(a)\sqrt{\rho^2-\ell_{1k}^2(a)}\right)+2\bar{f}\bar{M}\,e^{i3\phi}\frac{1}{3\rho^3}\left\{4z_k(2a^3-[2a^2+\ell_{1k}^2(a)]\sqrt{a^2-\ell_{1k}^2(a)})\right.$$
$$\left.\left.-3\ell_{1k}^3(a)\sqrt{\rho^2-\ell_{1k}^2(a)}\right\}\right]-\frac{3i\gamma_3}{16\pi a^3 A_{44}}\left[(f\bar{M}\,e^{i\phi}-fM\,e^{-i\phi}+\bar{f}M\,e^{i\phi})\left(\rho\sin^{-1}\frac{\ell_{13}(a)}{\rho}\right.\right.$$

$$-\frac{1}{\rho}\ell_{13}(a)\sqrt{\rho^2-\ell_{13}^2(a)}\Big)-2\bar{f}\bar{M}\,\mathrm{e}^{i3\phi}\frac{1}{3\rho^3}\Big\{4z_3(2a^3-[2a^2+\ell_{13}^2(a)]\sqrt{a^2-\ell_{13}^2(a)})$$

$$-3\ell_{13}^3(a)\sqrt{\rho^2-\ell_{13}^2(a)}\Big\}\Big], \tag{30}$$

$$w=\frac{3Hi\gamma_1\gamma_2}{4a^3}\sum_{k=1}^{2}\frac{m_k}{(m_k-1)\gamma_k}\Big[(fM-f\bar{M})\Big(z_k\sin^{-1}\frac{\ell_{1k}(a)}{\rho}-\sqrt{a^2-\ell_{1k}^2(a)}\Big)$$

$$+(fM\,\mathrm{e}^{-i2\phi}-\bar{f}\bar{M}\,\mathrm{e}^{i2\phi})\frac{1}{3\rho^2}(2a^3-[2a^2+\ell_{1k}^2(a)]\sqrt{a^2-\ell_{1k}^2(a)})\Big], \tag{31}$$

$$\sigma_1=\frac{3HiA_{66}\gamma_1\gamma_2}{2a^3}\sum_{k=1}^{2}\frac{[\gamma_k^2-(1+m_k)\gamma_3^2]}{\gamma_k^2(m_k-1)}\Big[(\bar{f}M-f\bar{M})\Big(\sin^{-1}\frac{\ell_{1k}(a)}{\rho}$$

$$-\frac{a\ell_{2k}(a)\sqrt{\rho^2-\ell_{1k}^2(a)}}{\rho[\ell_{2k}^2(a)-\ell_{1k}^2(a)]}\Big)+(\bar{f}\bar{M}\,\mathrm{e}^{i2\phi}-fM\,\mathrm{e}^{-i2\phi})\frac{\ell_{1k}^3(a)\sqrt{\rho^2-\ell_{1k}^2(a)}}{\rho^2[\ell_{2k}^2(a)-\ell_{1k}^2(a)]}\Big], \tag{32}$$

$$\sigma_2=\frac{3HiA_{66}\gamma_1\gamma_2}{2a^3}\sum_{k=1}^{2}\frac{1}{(m_k-1)}\Big[(\bar{f}M\,\mathrm{e}^{i2\phi}-f\bar{M}\,\mathrm{e}^{i2\phi}-\bar{f}\bar{M}\,\mathrm{e}^{i4\phi})\frac{\ell_{1k}^3(a)\sqrt{\rho^2-\ell_{1k}^2(a)}}{\rho^2[\ell_{2k}^2(a)-\ell_{1k}^2(a)]}$$

$$-fM\Big(\sin^{-1}\frac{\ell_{1k}(a)}{\rho}-\frac{a\ell_{2k}(a)\sqrt{\rho^2-\ell_{1k}^2(a)}}{\rho[\ell_{2k}^2(a)-\ell_{1k}^2(a)]}\Big)$$

$$+\bar{f}\bar{M}\,\mathrm{e}^{i4\phi}\frac{1}{\rho^4}\Big\{6\ell_{1k}^3(a)\sqrt{\rho^2-\ell_{1k}^2(a)}-8z_k(2a^3-[2a^2+\ell_{1k}^2(a)]\sqrt{a^2-\ell_{1k}^2(a)})\Big\}\Big]$$

$$+\frac{3i}{4\pi a^3\gamma_3}\Big[(\bar{f}M\,\mathrm{e}^{i2\phi}+f\bar{M}\,\mathrm{e}^{i2\phi}-\bar{f}\bar{M}\,\mathrm{e}^{i4\phi})\frac{\ell_{13}^3(a)\sqrt{\rho^2-\ell_{13}^2(a)}}{\rho^2[\ell_{23}^2(a)-\ell_{13}^2(a)]}$$

$$+fM\Big(\sin^{-1}\frac{\ell_{13}(a)}{\rho}-\frac{a\ell_{23}(a)\sqrt{\rho^2-l_{13}^2(a)}}{\rho[\ell_{23}^2(a)-\ell_{13}^2(a)]}\Big)$$

$$+\bar{f}\bar{M}\,\mathrm{e}^{i4\phi}\frac{1}{\rho^4}\Big\{6\ell_{13}^3(a)\sqrt{\rho^2-\ell_{13}^2(a)}-8z_3(2a^3-[2a^2+\ell_{13}^2(a)]\sqrt{a^2-\ell_{13}^2(a)})\Big\}\Big], \tag{33}$$

$$\sigma_{zz}=\frac{3i\gamma_1\gamma_2}{8\pi a^3(\gamma_1-\gamma_2)}\sum_{k=1}^{2}(-1)^{k+1}\Big[(\bar{f}M-f\bar{M})\Big(\sin^{-1}\frac{\ell_{1k}(a)}{\rho}$$

$$-\frac{a\ell_{2k}(a)\sqrt{\rho^2-\ell_{1k}^2(a)}}{\rho[\ell_{2k}^2(a)-\ell_{1k}^2(a)]}\Big)+(\bar{f}\bar{M}\,\mathrm{e}^{i2\phi}-fM\,\mathrm{e}^{-i2\phi})\frac{\ell_{1k}^3(a)\sqrt{\rho^2-\ell_{1k}^2(a)}}{\rho^2[\ell_{2k}^2(a)-\ell_{1k}^2(a)]}\Big]. \tag{34}$$

$$\tau_z=\frac{3i\gamma_1\gamma_2}{8\pi a^3(\gamma_1-\gamma_2)}\sum_{k=1}^{2}\frac{(-1)^{k+1}}{\gamma_k}\Big[(fM\,\mathrm{e}^{-i\phi}-f\bar{M}\,\mathrm{e}^{i\phi}+\bar{f}M\,\mathrm{e}^{i\phi}$$

$$-\bar{f}\bar{M}\,\mathrm{e}^{i3\phi})\frac{\ell_{1k}^2(a)\sqrt{a^2-\ell_{1k}^2(a)}}{\rho[\ell_{2k}^2(a)-\ell_{1k}^2(a)]}+\bar{f}\bar{M}\,\mathrm{e}^{i3\phi}\frac{4}{3\rho^3}(2a^3-[2a^2+\ell_{1k}^2(a)]\sqrt{a^2-\ell_{1k}^2(a)})\Big]$$

$$+\frac{3i}{8\pi a^3}\Big[(f\bar{M}\,\mathrm{e}^{i\phi}-fM\,\mathrm{e}^{-i\phi}+\bar{f}M\,\mathrm{e}^{i\phi}-\bar{f}\bar{M}\,\mathrm{e}^{i3\phi})\frac{\ell_{13}^2(a)\sqrt{a^2-\ell_{13}^2(a)}}{\rho[\ell_{23}^2(a)-\ell_{13}^2(a)]}$$

$$+\bar{f}\bar{M}\,\mathrm{e}^{i3\phi}\frac{4}{3\rho^3}(2a^3-[2a^2+\ell_{13}^2(a)]\sqrt{a^2-\ell_{13}^2(a)})\Big]. \tag{35}$$

5. DISCUSSION

It was noted earlier that the above solutions for shear loading are approximate since the tangential displacements will not generally align to oppose relative motion. The tangential traction will also produce a normal displacement in the contact region thus altering the contact pressure. To consider these details further the surface displacements in the contact region will be examined. For evaluating the surface conditions the following limits are useful:

$$\lim_{z\to 0} \ell_1(a) = \min(a,\rho), \quad \lim_{z\to 0} \ell_2(a) = \max(a,\rho), \tag{36}$$

where $\min(a,\rho)$ is the minimum of the two values and $\max(a,\rho)$ the maximum. The above limits are also valid for $\ell_{1k}(a)$ and $\ell_{2k}(a)$ since $z \to 0$ implies $z_k \to 0$ as well.

Consider first the sliding upright indenter. From eqns (16, 17) one may obtain:

$$u^c = \frac{fP\pi}{4a} G_1, \quad \rho < a, \tag{37}$$

$$w = \frac{HP\alpha}{a}(f_x \cos\phi + f_y \sin\phi)\frac{a-\sqrt{a^2-\rho^2}}{\rho}, \quad \rho < a, \tag{38}$$

where the elastic constants β, α, G_1 and G_2 are defined as (Fabrikant, 1989)

$$\beta = \frac{\gamma_3}{2\pi A_{44}}, \quad G_1 = \beta + \gamma_1\gamma_2 H, \quad G_2 = \beta - \gamma_1\gamma_2 H,$$

$$\alpha = \gamma_1\gamma_2 \sum_{k=1}^{2} \frac{m_k}{(m_k-1)\gamma_k} = \frac{\sqrt{A_{11}A_{33}} - A_{13}}{A_{11}(\gamma_1+\gamma_2)}, \tag{39}$$

and they are all real quantities. From eqn (37) it is apparent that f is the only complex quantity on the right hand side and therefore one can write $u^c = u + iv = C(f_x + if_y)$ where C is a real constant. In this case the tangential displacement does align with the direction of shear traction and the solution is exact in this sense for any transversely isotropic material. Equation (38) reveals that the normal displacement in the contact region is non-zero and this will alter the contact pressure. It has a maximum value at $\rho = a$ and vanishes for $\rho = 0$. In the special case of $\alpha = 0$ the normal displacement vanishes everywhere on the surface and there is no interaction. For isotropy $\alpha = ((1-2\nu)/2(1-\nu))$ where ν is Poisson's ratio and thus $\alpha = 0$ corresponds to an incompressible material. It may now be concluded that the solution derived here for a sliding upright indenter is an exact solution for materials with $\alpha = 0$. For $\alpha \neq 0$ the shear stress and tangential displacement are still in alignment but the solution is not exact since the shear loading will alter the contact pressure.

Now considering the tilted indenter, from eqns (30, 31) the surface displacements in the loaded region are:

$$u^c = \frac{3\pi}{8a^3} f(yM_x - xM_y)G_1 - \frac{3i\pi}{16a^3} \bar{f}M(x+iy)G_2, \quad \rho < a, \tag{40}$$

$$w = \frac{3iH\alpha}{4a^3}\left[-(\bar{f}M - f\bar{M})\sqrt{a^2-\rho^2} + (fM\, e^{-i2\phi} - \bar{f}\bar{M}\, e^{i2\phi})\frac{1}{3\rho^2} \times (2a^3 - (2a^2+\rho^2)\sqrt{a^2-\rho^2}) \right], \quad \rho < a. \tag{41}$$

It is apparent in this case that the tangential displacements do not align with the shear traction. This results from the coupling of the second term in eqn (40). In the special case

$G_2 = 0$ the coupling vanishes and the displacements and tractions align. For isotropy this corresponds to $\nu = 0$. The normal displacement is also nonzero except when α vanishes. For a transversely isotropic material there are five elastic constants and it may be possible for α and G_2 to be zero simultaneously, thus yielding an exact solution for a sliding tilted indenter. An isotropic material can not have $\nu = 0$ and $\nu = \frac{1}{2}$ simultaneously and thus the solution must be judged as approximate in this case.

6. APPLICATIONS TO FRACTURE MECHANICS

The relevance of one of the solutions derived here to the area of fracture mechanics is now pointed out. Consider an infinite transversely isotropic body $-\infty < z < \infty$ with a circular external crack on the plane $z = 0$. The crack plane is parallel to the planes of isotropy and the crack occupies the region $\rho > a$. Assume that for $z = -\infty$ the displacements $u^c = u^c_\infty = u_\infty + iv_\infty$ are imposed while for $z = +\infty$ the displacements are $u^c = -u^c_\infty$, where u^c_∞ is a constant. The $z = 0$ plane is then one of anti-symmetry. The problem is equivalent to one for the half space $z > 0$ (Fig. 1) with the boundary conditions

$$\begin{aligned} \sigma_{zz}(\rho, \phi, 0) &= 0, \quad 0 < \rho < \infty, \\ \tau_z(\rho, \phi, 0) &= 0, \quad a < \rho < \infty, \\ u^c(\rho, \phi, 0) &= 0, \quad 0 < \rho < a, \\ \lim_{z \to \infty} u^c(\rho, \phi, z) &= -u^c_\infty, \quad \lim_{z \to \infty} w(\rho, \phi, z) = 0. \end{aligned} \tag{42}$$

Since one may add rigid body displacements without affecting the stress fields, the addition of the displacement u^c_∞ to the half space leads to the boundary conditions

$$\begin{aligned} \sigma_{zz}(\rho, \phi, 0) &= 0, \quad 0 < \rho < \infty, \\ \tau_z(\rho, \phi, 0) &= 0, \quad a < \rho < \infty, \\ u^c(\rho, \phi, 0) &= u^c_\infty, \quad 0 < \rho < a, \\ \lim_{z \to \infty} u^c(\rho, \phi, z) &= 0, \quad \lim_{z \to \infty} w(\rho, \phi, z) = 0. \end{aligned} \tag{43}$$

The elastic field to this boundary value problem is given in Section 3 for sliding flat indentation. Obviously the stress boundary conditions are satisfied and all displacements vanish for $z \to \infty$. The tangential surface displacement in the region $\rho < a$ is constant and given in eqn (37) as

$$u^c_\infty = \frac{fP\pi}{4a} G_1. \tag{44}$$

Thus if one substitutes $fP = (4au^c_\infty/\pi G_1)$ in the solution of Section 3, the stress fields for this external crack problem are obtained. The surface displacements and stresses for this problem agree with the result given by Fabrikant (1989). The displacement fields are obtained by the same substitution in addition to subtracting the rigid body displacement u^c_∞.

A few final comments are in order. It is noted that for the tilted indenter the net normal force, and thus the net tangential force, are both zero. By itself this solution has little physical significance. However, adding this solution with the solution for sliding of an upright indenter allows sliding of a noncentrally loaded flat circular punch to be analyzed. In addition it was pointed out earlier that the solutions here for shear loading must be added to the solutions given in Fabrikant (1988) for frictionless indentation to obtain the complete solution for indentation and sliding. The expressions for the elastic field for the tilted indenter given there contain two misprints. The eqn (67) for σ_2 should be multiplied

by a factor of 2 (the 2 should be replaced with a 4) while eqn (69) for τ_z should contain a $(-1)^{k+1}$ just to the right of the summation sign.

7. SOLUTIONS FOR ISOTROPY

All of the results in this paper have been derived for a transversely isotropic material. The solutions are given in terms of the material parameters γ_1, γ_2, γ_3, m_1, m_2, H, A_{44} and A_{66} which are defined by Fabrikant (1989) or see Hanson (1992a). To obtain the results for isotropy one must let the elastic parameters take on their equivalent isotropic values. For isotropy $H = [(1-\nu^2)/\pi E]$ and $A_{44} = A_{66} = (E/2(1+\nu))$ where E is Young's modulus and ν is Poisson's ratio. However for isotropy it is also true that $\gamma_1, \gamma_2, \gamma_3, m_1, m_2 \to 1$ (Fabrikant, 1989) and the denominators of the expressions for displacements and stresses tend to zero. A limiting procedure is thus required to extract the isotropic relations. The required isotropic limits needed for the shear loading considered here are:

$$\sum_{k=1}^{2} \frac{1}{(m_k-1)} f(z_k) = -f(z) - \frac{z}{2(1-\nu)} f'(z), \tag{45}$$

$$\sum_{k=1}^{2} \frac{m_k}{\gamma_k(m_k-1)} f(z_k) = \frac{(1-2\nu)f(z) - zf'(z)}{2(1-\nu)}, \tag{46}$$

$$\sum_{k=1}^{2} \frac{\gamma_k^2 - (1+m_k)\gamma_3^2}{\gamma_k^2(m_k-1)} f(z_k) = \frac{2(1+\nu)f(z) + zf'(z)}{2(1-\nu)}, \tag{47}$$

$$\frac{1}{\gamma_1-\gamma_2} \sum_{k=1}^{2} (-1)^{k+1} f(z_k) = -zf'(z), \tag{48}$$

$$\frac{1}{\gamma_1-\gamma_2} \sum_{k=1}^{2} \frac{(-1)^{k+1}}{\gamma_k} f(z_k) = -f(z) - zf'(z), \tag{49}$$

where $f'(z)$ denotes the derivative of $f(z)$ with respect to z.

8. NUMERICAL RESULTS

In this section some numerical results are given to illustrate the effects of transverse isotropy and shear loading on the internal stress fields. The only previous results given in the literature are those provided by Sneddon (1966) who derived closed form expressions for the elastic field for flat frictionless indentation of an isotropic half space and gave numerical values for subsurface stresses in tabular form. In the present numerical study the elastic fields for frictionless indentation obtained by Fabrikant (1988) were superposed with the results for shear loading presently derived.

The first step was to compare present calculations with Sneddon's results. It was found that in some cases the present numbers were in good agreement while in other cases there were significant discrepancies. To determine the cause of the disagreement, the analytical derivations in Sneddon's paper were repeated and several misprints in his formulas were found. In particular, his eqn (3) for the stress σ_θ contains two misprints and should read as follows

$$\sigma_\theta = -\frac{4\lambda\mu}{\lambda+2\mu}\frac{\varepsilon}{\pi a} J_1^o - \frac{4\mu^2}{\rho(\lambda+2\mu)}\frac{\varepsilon}{\pi a}\left(J_o^1 - \frac{\lambda+\mu}{\mu}\zeta J_1^1\right). \tag{50}$$

Also his eqn (16) for J_2^o should be

$$J_2^v = rR^{-3/2} \sin(\tfrac{3}{2}\phi - \theta). \tag{51}$$

Using the corrected forms of Sneddon's expressions led to numerical results which were in perfect agreement with the current numerical results. It was thus concluded that some error occurred in performing the numerical evaluations in Sneddon's tables and some of these numerical results should be disregarded.

The remainder of this section presents new numerical results for the subsurface stress fields resulting from flat indentation with sliding. First the axisymmetric frictionless case is examined and Fig. 2 plots contours of the maximum shear stress for an isotropic material with $\nu = 0.3$. In all stress plots the stress is nondimensionlized by dividing by the average contact stress $\sigma_{av} = P/(\pi a^2)$. Figure 3 displays the analogous result for Cadmium which is a transversely isotropic material. The elastic constants for Cadmium are given as $A_{11} = 109.21$ GPa, $A_{13} = 37.55$ GPa, $A_{33} = 46.03$ GPa, $A_{44} = 15.63$ GPa and $A_{66} = 34.72$ GPa which were obtained from the paper by Dahan and Zarka (1977), and are close to similar values given by Zureick and Eubanks (1988). The maximum shear stress was chosen to plot since it is a quantity which can be related to the yielding behavior for ductile materials and the von-Mises yield criterion may not be applicable to nonisotropic materials as discussed by Hill (1950). It was found that the hoop stress was almost always the middle principal stress and thus the maximum shear stress was contained in the axisymmetric planes. From the results it is apparent that Figs 2 and 3 have similar features. This was not true for the Hertzian indentation studied by Dahan and Zarka (1977) whose results showed that the contours of Mises stress for Cadmium was significantly different than for isotropy. Since Hertzian contact produces no contact stress singularity, it can be concluded that the stress singularity present for the flat indenter at the edge of contact is the dominant factor in producing the maximum shear stress and it overwhelms any effect due to transverse isotropy. Presently the transverse isotropy gives only a shift in the contour level magnitude as compared to the isotropic results. The same comments apply to Figs 4 and 5 which plot τ_{max} in the x–z plane when sliding in the x direction is included using a friction coefficient of $f_x = 0.3$.

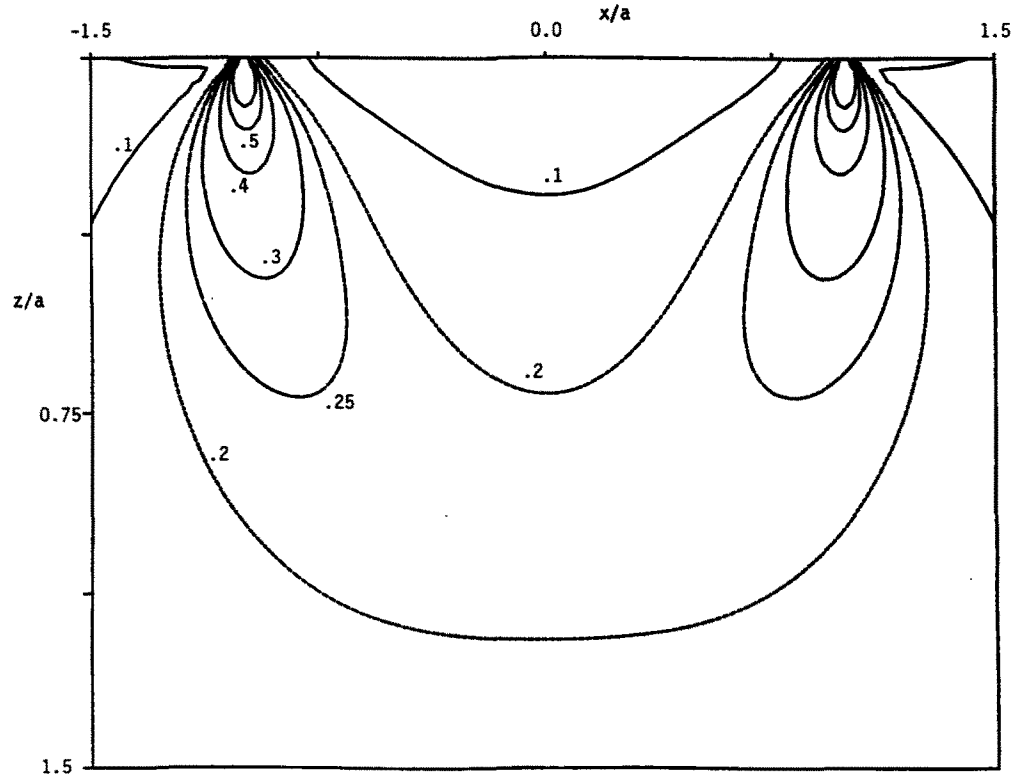

Fig. 2. Contours of τ_{max}/σ_{av} in the $y = 0$ plane for an isotropic material with $\nu = 0.3$, $f_x = f_y = 0$.

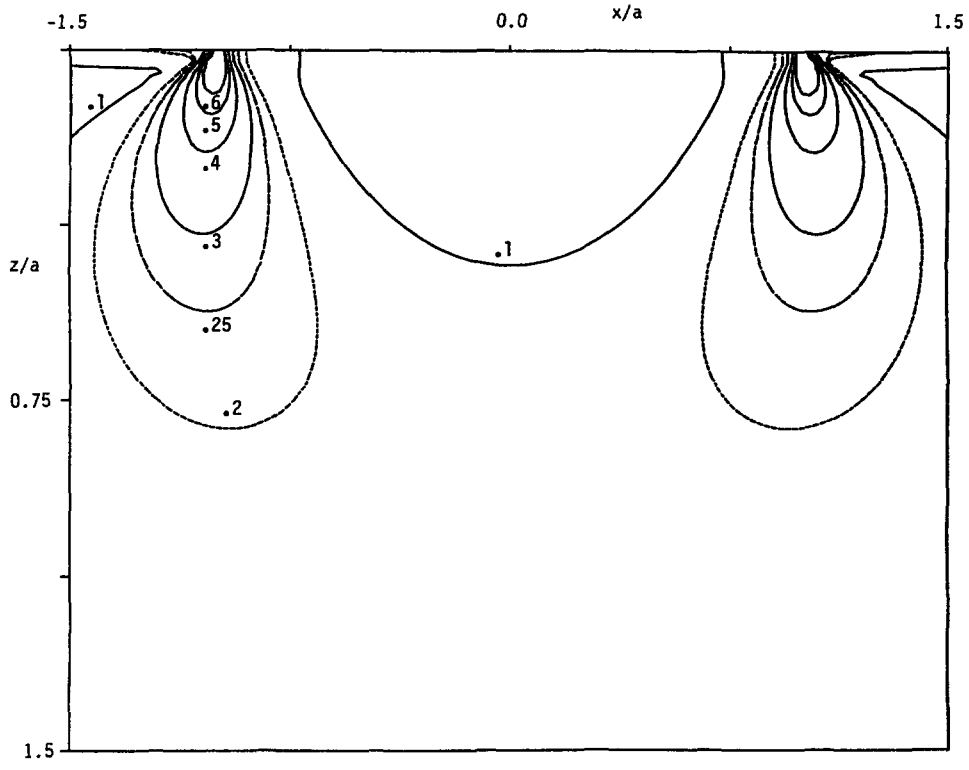

Fig. 3. Contours of τ_{max}/σ_{av} in the $y = 0$ plane for Cadmium, $f_x = f_y = 0$.

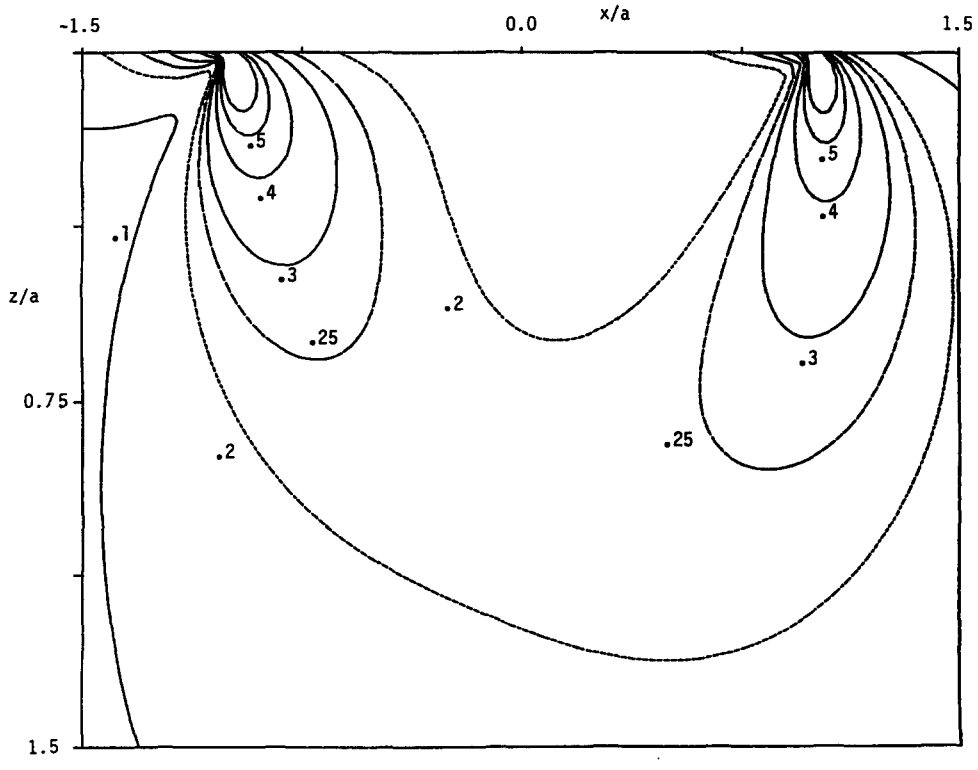

Fig. 4. Contours of τ_{max}/σ_{av} in the $y = 0$ plane for an isotropic material with $\nu = 0.3, f_x = 0.3, f_y = 0$.

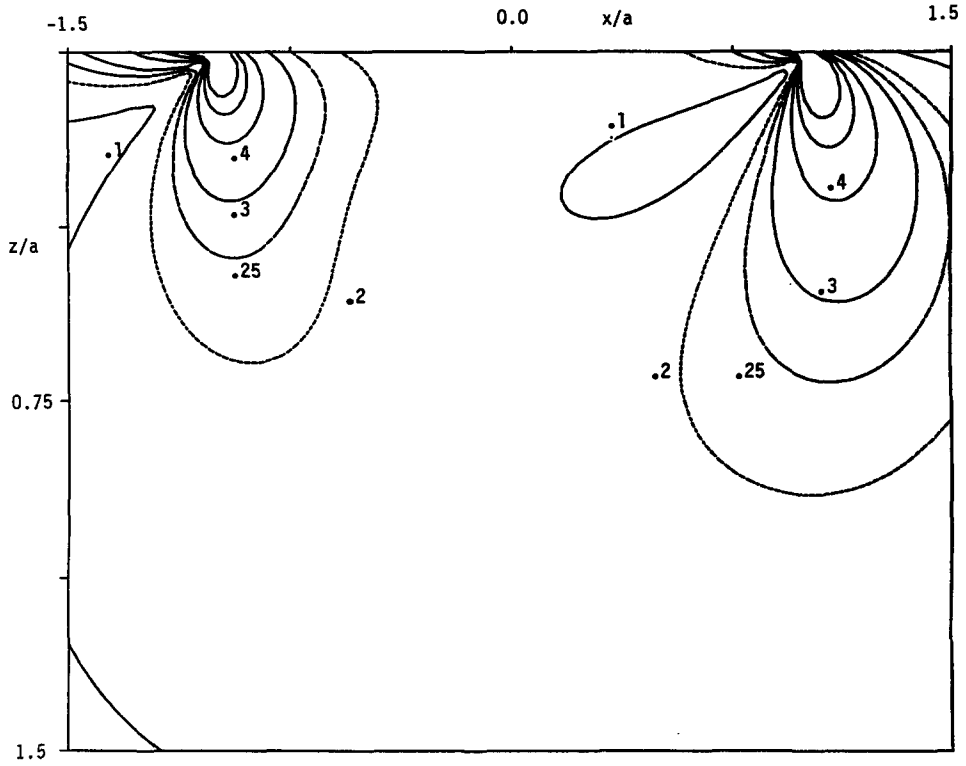

Fig. 5. Contours of τ_{max}/σ_{av} in the $y = 0$ plane for Cadmium, $f_x = 0.3$, $f_y = 0$.

In the remaining results attention is focused on the subsurface hoop stress which is pertinent to the investigation of subsurface cracking resulting from indentation of brittle materials. Other stress components can be investigated in a similar manner and will not be discussed here. From Figs 2–5 it might be assumed that transverse isotropy has only a small effect. However, the following figures indicate that this is not true. Figure 6 displays the subsurface hoop stress for flat frictionless indentation of an isotropic material. Under the indenter it is compression, tending to infinity at the edge of contact, while it becomes tensile at a larger depth with a maximum value of 0.005 at $x/a = 0.0$, $z/a = 3.0$. Similar results for Cadmium are presented in Fig. 7. Now it is apparent that the tensile stress region shifts off from the axis of contact and forms a doughnut shaped region encircling the indenter. The maximum value is now 0.01 at $x/a = 2.286$, $z/a = 1.2$ which is double the isotropic result. Results for a third transversely isotropic ceramic material, $BaTiO_3$, are shown in Fig. 8. In this case the maximum is back below the indenter with a value of 0.063 at $x/a = 0.0$, $z/a = 1.71$ which is much larger and closer to the surface than the isotropic result. As indicated in Fig. 9, the compressive hoop stress is also significantly altered by transverse isotropy. Along the z axis the hoop stresses reach a value of -0.6 at the surface which is 50% larger than the isotropic value of -0.4.

The final two figures display the effect of shear loading and transverse isotropy on subsurface hoop stresses. Using a friction coefficient of 0.5 for sliding in the x direction, Fig. 10 presents the results for isotropy while Fig. 11 is for Cadmium. Comparing Fig. 10 to Fig. 6 it is obvious that shear loading creates some asymmetry in the subsurface stresses and gives a slightly larger tensile stress magnitude of 0.0056. Fig. 11 for Cadmium illustrates how transverse isotropy greatly enhances the asymmetry caused by shear loading. Comparing to Fig. 7 it can be seen that the tensile stress ahead of the shear loading is greatly increased to a value of 0.0167 while it is reduced behind the loading to the 0.0069. The near surface compressive stresses appear to be less affected by shear loading.

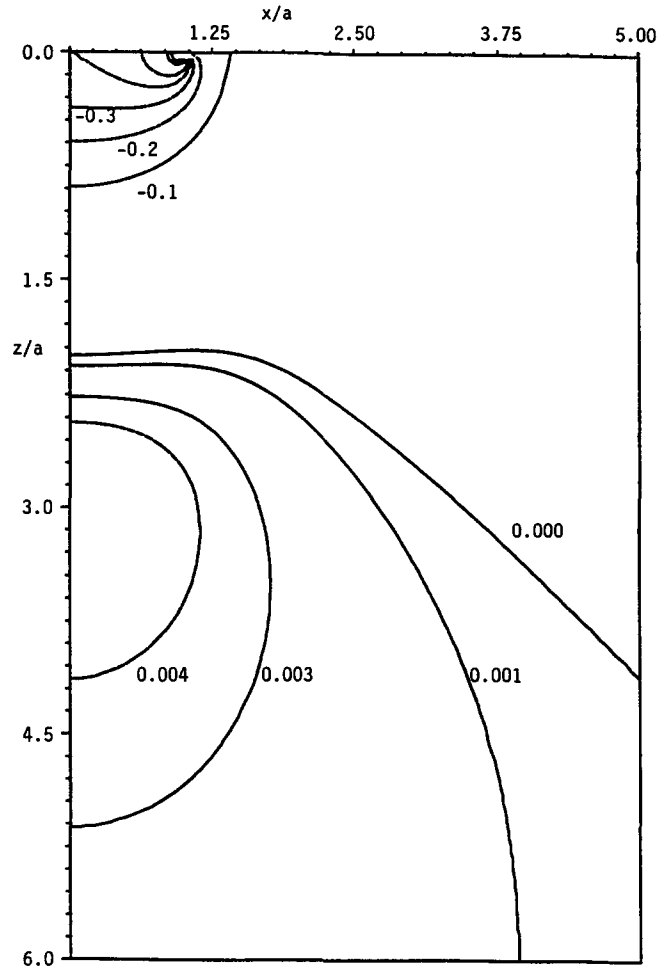

Fig. 6. Contours of σ_{yy}/σ_{av} in the $y = 0$ plane for an isotropic material with $\nu = 0.3$, $f_x = f_y = 0$.

9. CONCLUSIONS

The present research has provided closed form solutions to the elastic field resulting from sliding of a flat or inclined cylindrical indenter. The solutions are generally approximate since the alteration of the contact pressure resulting from shear loading was neglected and also the shear stresses do not completely align with the direction of relative displacement. However, it was shown that under certain conditions this interaction vanishes ($\alpha = 0$) and shear loading produces no normal displacement on the surface. Also for the flat indenter the displacements do align with the shear traction for all elastic constants and thus under these conditions the present solution is exact.

Even for cases when $\alpha \neq 0$, the interaction is not a dominant factor. For example from eqn (38) the maximum normal displacement at the edge of contact is $w = HP\alpha f_x/a$ when shear loading is in the x direction whereas the normal displacement resulting from normal loading is $PH\pi/(2a)$. The ratio of maximum normal displacement caused by sliding to that caused by indentation is $2\alpha f_x/\pi$. For an isotropic material this becomes $(1-2\nu)f_x/[\pi(1-\nu)]$. If $\nu = 0.3$ and $f_x = 0.3$ this ratio becomes 0.05 and thus the normal displacement caused by shear loading is only 5% of the direct indentation displacement in the worst case. This point can also be viewed by considering the two-dimensional analogue of this problem. For sliding in the x direction the contact pressure for the flat indenter along the center should have a form similar to the two-dimensional distribution. The plane strain contact stress including the interaction is given as

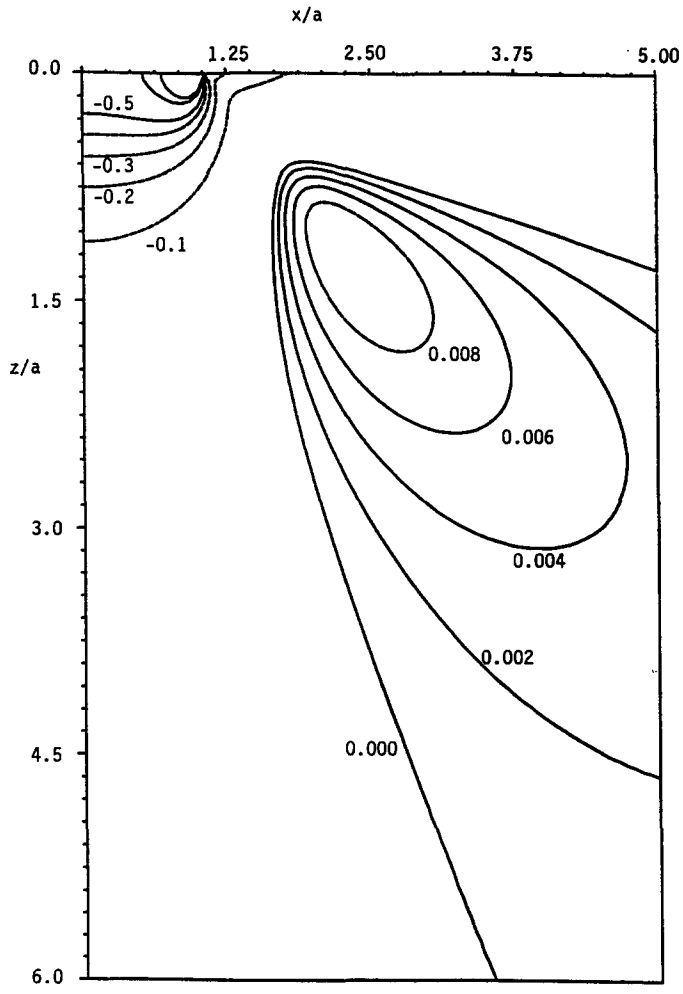

Fig. 7. Contours of σ_{yy}/σ_{av} in the $y = 0$ plane for Cadmium, $f_x = f_y = 0$.

$$\sigma_{zz} = -\left(\cos(\pi\alpha)\left(\frac{a-x}{a+x}\right)^{\alpha}\right)\frac{P}{\pi\sqrt{a^2-x^2}}, \quad \alpha = \frac{1}{\pi}\tan^{-1}\left(f\frac{\kappa-1}{\kappa+1}\right), \tag{52}$$

where f is the friction coeffficient and $\kappa = 3-4\nu$. The effect of friction is to alter the order of the stress singularity at the edges of contact. For $f = 0$, $\alpha = 0$ and the frictionless result is obtained. If the frictional effect in brackets is calculated for $f = \nu = 0.3$, then $\alpha = 0.0272$ and a simple calculation reveals that the true stress and the frictionless stress differ by less than 3% in the region $-0.5a < x < 0.5a$. The difference at $x = 0.93a$ is only 9%. Therefore the only significant deviation occurs at the extreme edges of contact. Since the net force is identical in each case, neglecting the interaction will only give any significant error at the edge of contact. Away from the edge and in the subsurface region the frictionless results should be a good approximation due to St Venant's principle. A comparison of the surface shear stress will lead to the same conclusion since it is just a constant multiple of the surface normal stress. Therefore the present closed form solutions provide a very good representation for the elastic field in a manner amenable to simple calculations.

The numerical results were illustrated by plotting subsurface stress fields. It was found that the maximum shear stress occurred at the edge of contact, increasing in an unbounded manner. The maximum shear stress distribution was relatively unaffected by transverse isotropy. One can thus conclude that the stress singularity at the contact edge dominates the stress field distribution in the region close to the contact. On the other hand, it was also shown that the subsurface hoop stress distribution was significantly altered by material

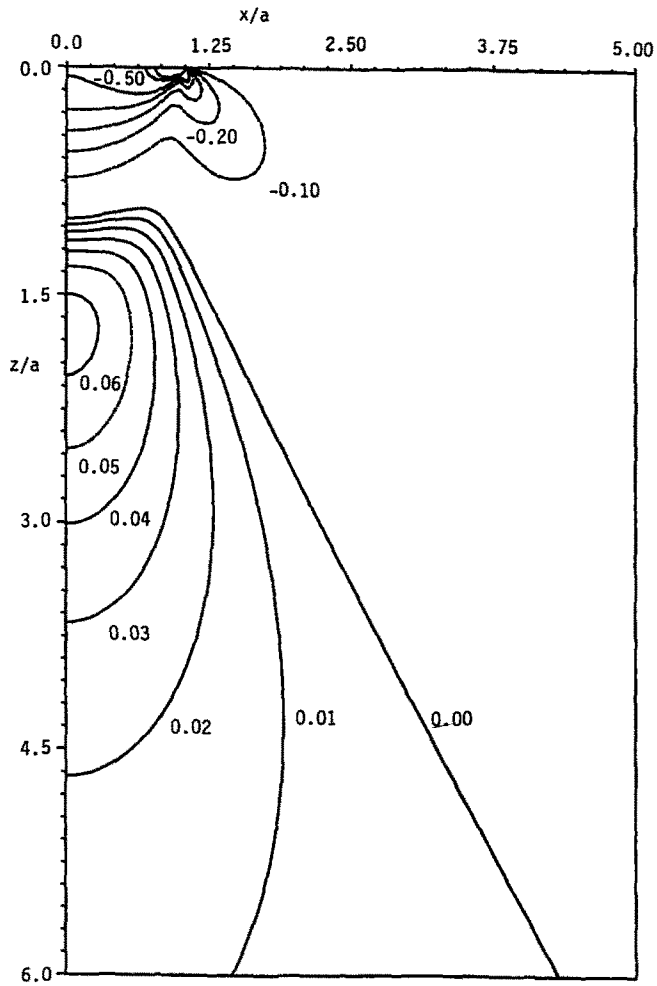

Fig. 8. Contours of σ_{yy}/σ_{av} in the $y = 0$ plane for $BaTiO_3$, $f_x = f_y = 0$.

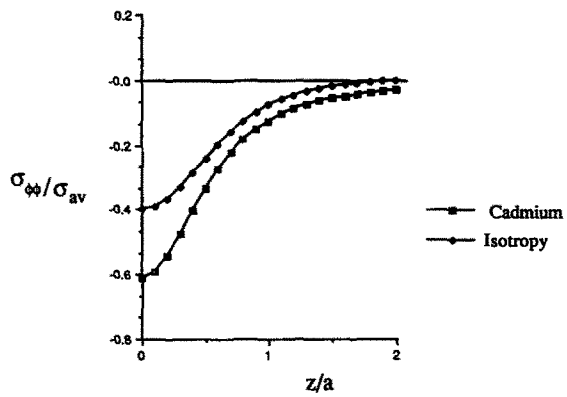

Fig. 9. Comparison of the hoop stress along the z axis for an isotropic and a tranversely isotropic material, frictionless indentation case.

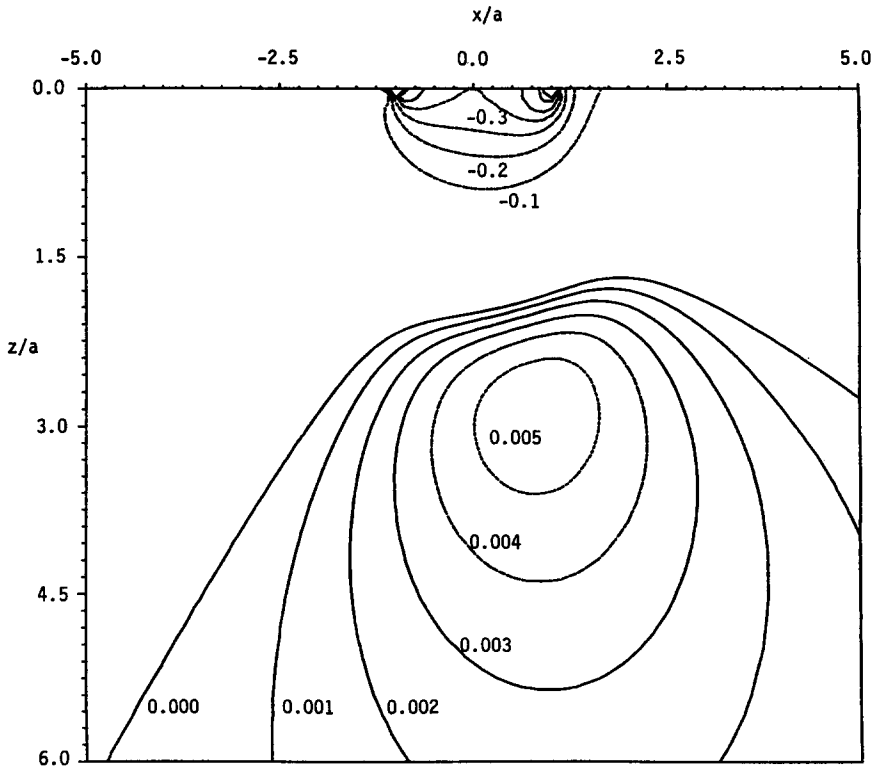

Fig. 10. Contours of σ_{yy}/σ_{av} in the $y = 0$ plane for an isotropic material with $\nu = 0.3, f_x = 0.5, f_y = 0$.

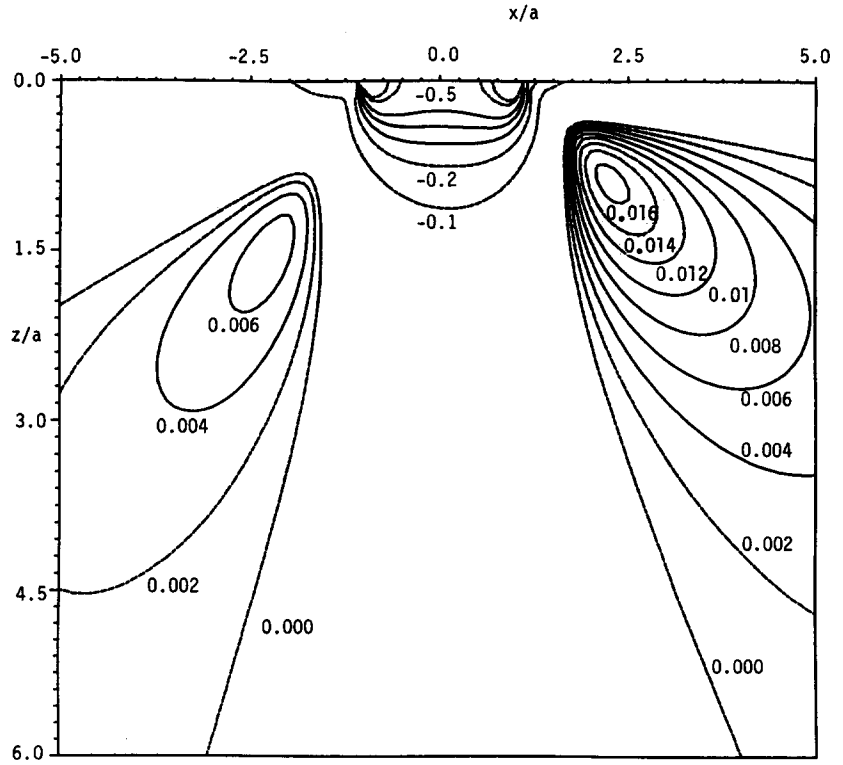

Fig. 11. Contours of σ_{yy}/σ_{av} in the $y = 0$ plane for Cadmium, $f_x = 0.3, f_y = 0$.

anisotropy. Transverse isotropy increased the maximum value and in some instances also shifted its location to a point off the axis of contact. Finally, shear loading for isotropy gave a small alteration in the hoop stress while the effect of shear for transverse isotropy was more pronounced.

Acknowledgement—It is gratefully acknowledged that this research was partially supported by the National Science Foundation under grant No. MSS-9210531.

REFERENCES

Dahan, M. and Zarka, J. (1977) Elastic contact between a sphere and a semi infinite transversely isotropic body. *Int. J. Solids Structures* **13,** 229–238.

Elliot, H. A. (1949). Axial symmetric stress distributions in aeolotropic hexagonal crystals. The problem of the plane and related problems. *Proc. Cambridge Philosophical Society.* **45,** 621–630.

Fabrikant, V. I. (1988) Elastic field around a circular punch. *ASME J. Appl. Mech.* **55,** 604–610.

Fabrikant, V. I. (1989) *Applications of Potential Theory in Mechanics: A Selection of New Results.* pp. 71–79, 110–111. Kluwer Academic Publishers, The Netherlands.

Gladwell, G. M. L. (1980). *Contact Problems in the Classical Theory of Elasticity.* Sijthoff & Noordhoff, The Netherlands.

Hanson, M. T. (1992a). The elastic field for conical indentation including sliding friction for transverse isotropy. *ASME J. Appl. Mech.* **59,** S123–S130.

Hanson, M. T. (1992b) The elastic field for spherical hertzian contact including sliding friction for transverse isotropy. *ASME J. Tribology* **114,** 606–611.

Hanson, M. T. (1993a). The elastic field for a conical punch sliding on an isotropic half space. *ASME J. Appl. Mech.* **60**(2), 557–559.

Hanson, M. T. and Johnson, T. (1993b) The elastic field for spherical hertzian contact of isotropic bodies revisited: some alternative expressions. *ASME J. Tribology* **115,** 327–332.

Hill, R. (1950). *The Mathematical Theory of Plasticity.* pp. 318–320. Oxford University Press.

Mindlin, R. D. (1949). Compliance of Elastic Bodies in Contact. *ASME J. Appl. Mech.* **16,** 259–268.

Muki, R. (1960) Asymmetric problems of the theory of elasticity for a semi-infinite solid and a thick plate. In *Progress in Solid Mechanics* (Edited by I. N. Sneddon and R. Hill), pp. 401–439. North Holland, Amsterdam.

Sneddon, I. N. (1946). Boussinesq's problem for a flat-ended cylinder. *Proc. Cambridge Philosophical Society* **42,** 29–39.

Watson, G. N. (1980) *A Treatise on the Theory of Bessel Functions.* Chapter 13. Cambridge University Press.

Westmann, R. A. (1965). Asymmetric mixed boundary value problems of the elastic half space. *ASME J. Appl. Mech.* **32,** 411–417.

Zureick, A. H. and Eubanks, R. A. (1988) Spheroidal cavity with prescribed asymmetric tractions in three-dimensional transverse isotropy. *ASCE J. Engng Mech.* **114,** 24–48.

APPENDIX A

The derivatives of the function $\psi(\rho, \phi, z)$ defined in eqns (11, 13) are given. Some can be extracted from the solution of Fabrikant (1988) while the others were derived here. The results are:

$$\frac{\partial}{\partial z}\psi(\rho,\phi,z) = 2\pi \sin^{-1}\frac{\ell_1(a)}{\rho}, \tag{A1}$$

$$\Lambda\psi(\rho,\phi,z) = 2\pi\, e^{i\phi}\left\{\frac{a}{\rho} - \frac{\sqrt{a^2-\ell_1^2(a)}}{\rho}\right\}, \tag{A2}$$

$$\Lambda^2\psi(\rho,\phi,z) = 2\pi\, e^{i2\phi}\left\{\frac{\sqrt{a^2-\ell_1^2(a)}}{[\ell_2^2(a)-\ell_1^2(a)]} - \frac{2a}{\rho^2} + \frac{2}{\rho^2}\sqrt{a^2-\ell_1^2(a)}\right\}, \tag{A3}$$

$$\frac{\partial^2}{\partial z^2}\psi(\rho,\phi,z) = -2\pi\frac{\sqrt{a^2-\ell_1^2(a)}}{[\ell_2^2(a)-\ell_1^2(a)]} \tag{A4}$$

$$\Delta\psi(\rho,\phi,z) = 2\pi\frac{\sqrt{a^2-\ell_1^2(a)}}{[\ell_2^2(a)-\ell_1^2(a)]}, \tag{A5}$$

$$\frac{\partial}{\partial z}\Lambda\psi(\rho,\phi,z) = -2\pi\, e^{i\phi}\frac{\ell_1(a)\sqrt{\rho^2-\ell_1^2(a)}}{\rho[\ell_2^2(a)-\ell_1^2(a)]}, \tag{A6}$$

$$\Lambda\Delta\psi(\rho,\phi,z) = 2\pi\rho\, e^{i\phi}\frac{\sqrt{a^2-\ell_1^2(a)}}{[\ell_2^2(a)-\ell_1^2(a)]^3}(4a^2-\ell_1^2(a)-3\ell_2^2(a)), \tag{A7}$$

$$\Lambda^3\psi(\rho,\phi,z)=2\pi\,e^{i3\phi}\left\{\frac{8a}{\rho^3}-\frac{8}{\rho^3}\sqrt{a^2-\ell_1^2(a)}-\frac{4\sqrt{a^2-\ell_1^2(a)}}{\rho[\ell_2^2(a)-\ell_1^2(a)]}+\frac{\rho\sqrt{a^2-\ell_1^2(a)}}{[\ell_2^2(a)-\ell_1^2(a)]^3}(4a^2-\ell_1^2(a)-3\ell_2^2(a))\right\},\quad\text{(A8)}$$

where $\ell_1(a)$ and $\ell_2(a)$ are defined in eqns (24).

APPENDIX B

Here the function $\Phi(\rho,\phi,z)$ defined in eqn (12) is evaluated. First differentiation of eqn (12) with respect to z yields

$$\frac{\partial}{\partial z}\Phi(\rho,\phi,z)=z\int_0^{2\pi}\int_0^a\frac{1}{\sqrt{a^2-\rho_o^2}}\frac{1}{R}\rho_o\,d\rho_o\,d\phi_o=z\frac{\partial}{\partial z}\psi(\rho,\phi,z).\quad\text{(B1)}$$

Substituting from eqn (A1) and then integrating with respect to z results in:

$$\Phi(\rho,\phi,z)=\frac{\pi}{2}\left\{(2a^2+2z^2+\rho^2)\sin^{-1}\frac{\ell_1(a)}{\rho}+\frac{1}{a}(2a^2+\ell_1^2(a))\sqrt{\ell_2^2(a)-a^2}\right\}.\quad\text{(B2)}$$

Since the integral was evaluated as indefinite, an arbitrary function of the variables ρ, ϕ and a must be added. However, it can be shown by considering the behaviour at $z=\infty$ that this function is zero.

To evaluate the elastic field for shear loading, the relationship in eqn (B1) can be used along with the derivatives

$$\Delta\Phi(\rho,\phi,z)=2\pi\left\{\sin^{-1}\frac{\ell_1(a)}{\rho}+\frac{z\sqrt{a^2-\ell_1^2(a)}}{[\ell_2^2(a)-\ell_1^2(a)]}\right\},\quad\text{(B3)}$$

$$\Lambda^2\Phi(\rho,\phi,z)=-2\pi\,e^{2i\phi}\frac{\ell_1(a)[\rho^2-\ell_1^2(a)]^{3/2}}{\rho^2[\ell_2^2(a)-\ell_1^2(a)]},\quad\text{(B4)}$$

$$\Lambda\Delta\Phi(\rho,\phi,z)=2\pi\,e^{i\phi}\left\{-\frac{\ell_1(a)\sqrt{\rho^2-\ell_1^2(a)}}{\rho[\ell_2^2(a)-\ell_1^2(a)]}+\frac{z\rho\sqrt{a^2-\ell_1^2(a)}}{[\ell_2^2(a)-\ell_1^2(a)]^3}(4a^2-\ell_1^2(a)-3\ell_2^2(a))\right\},\quad\text{(B5)}$$

$$\Lambda^3\Phi(\rho,\phi,z)=2\pi\,e^{i3\phi}\left\{\frac{\ell_1(a)\sqrt{\rho^2-\ell_1^2(a)}}{\rho^3[\ell_2^2(a)-\ell_1^2(a)]}(3\rho^2-4\ell_1^2(a))+\frac{z\rho\sqrt{a^2-\ell_1^2(a)}}{[\ell_2^2(a)-\ell_1^2(a)]^3}(4a^2-\ell_1^2(a)-3\ell_2^2(a))\right\}.\quad\text{(B6)}$$

APPENDIX C

The derivatives of the potential function $\psi(\rho,\phi,z)$ defined in eqns (26, 28) are given as:

$$\frac{\partial}{\partial z}\psi(\rho,\phi,z)=\frac{\pi i}{2}(M\rho\,e^{-i\phi}-\bar{M}\rho\,e^{i\phi})\left\{\sin^{-1}\frac{\ell_1(a)}{\rho}-\frac{1}{\rho^2}\ell_1(a)\sqrt{\rho^2-\ell_1^2(a)}\right\},\quad\text{(C1)}$$

$$\Lambda\psi(\rho,\phi,z)=iM\pi\left(z\sin^{-1}\frac{\ell_1(a)}{\rho}-\sqrt{a^2-\ell_1^2(a)}\right)-i\pi\bar{M}\,e^{i2\phi}\frac{1}{3\rho^2}(2a^3-[2a^2+\ell_1^2(a)]\sqrt{a^2-\ell_1^2(a)}),\quad\text{(C2)}$$

$$\Lambda^2\psi(\rho,\phi,z)=i\pi(M\,e^{i\phi}-\bar{M}\,e^{i3\phi})\frac{\ell_1^2(a)\sqrt{a^2-\ell_1^2(a)}}{\rho[\ell_2^2(a)-\ell_1^2(a)]}+i\pi\bar{M}\,e^{i3\phi}\frac{4}{3\rho^3}(2a^3-[2a^2+\ell_1^2(a)]\sqrt{a^2-\ell_1^2(a)}),\quad\text{(C3)}$$

$$\frac{\partial^2}{\partial z^2}\psi(\rho,\phi,z)=i\pi(\bar{M}\rho\,e^{i\phi}-M\rho\,e^{-i\phi})\frac{\ell_1^2(a)\sqrt{a^2-\ell_1^2(a)}}{\rho^2[\ell_2^2(a)-\ell_1^2(a)]},\quad\text{(C4)}$$

$$\Delta\psi(\rho,\phi,z)=-i\pi(\bar{M}\rho\,e^{i\phi}-M\rho\,e^{-i\phi})\frac{\ell_1^2(a)\sqrt{a^2-\ell_1^2(a)}}{\rho^2[\ell_2^2(a)-\ell_1^2(a)]},\quad\text{(C5)}$$

$$\frac{\partial}{\partial z}\Lambda\psi(\rho,\phi,z)=iM\pi\left(\sin^{-1}\frac{\ell_1(a)}{\rho}-\frac{a\ell_2(a)\sqrt{\rho^2-\ell_1^2(a)}}{\rho[\ell_2^2(a)-\ell_1^2(a)]}\right)+i\pi\bar{M}\,e^{i2\phi}\frac{\ell_1^3(a)\sqrt{\rho^2-\ell_1^2(a)}}{\rho^2[\ell_2^2(a)-\ell_1^2(a)]}.\quad\text{(C6)}$$

The derivative $\Lambda^3\psi(\rho,\phi,z)$ is in a more complicated form and thus it is not given explicitly here. Only the combination $\Lambda^3(z\psi(\rho,\phi,z)-\Phi(\rho,\phi,z))$ is needed and this is given in Appendix D.

APPENDIX D

The function $\Phi(\rho,\phi,z)$ defined in eqn (27) is evaluated presently. Differentiation of eqn (27) with respect to z yields

$$\frac{\partial}{\partial z}\Phi(\rho,\phi,z) = z\,Im\left\{\bar{M}\int_0^{2\pi}\int_0^a \frac{\rho_o\,e^{i\phi_o}}{\sqrt{a^2-\rho_o^2}}\frac{1}{R}\rho_o\,d\rho_o\,d\phi_o\right\} = z\frac{\partial}{\partial z}\psi(\rho,\phi,z). \tag{D1}$$

Substituting from eqn (C1) and then integrating with respect to z results in

$$\Phi(\rho,\phi,z) = \frac{\pi i}{2}(M\rho\,e^{-i\phi}-\bar{M}\rho\,e^{i\phi})\left\{\tfrac{1}{8}(\rho^2+4z^2-4a^2)\sin^{-1}\frac{\ell_1(a)}{\rho}\right.$$
$$\left.-(\ell_1^2(a)+2\ell_2^2(a)-\tfrac{3}{2}\rho^2)\frac{\ell_1(a)\sqrt{\rho^2-\ell_1^2(a)}}{4\rho^2}\right\}. \tag{D2}$$

Since the integral was evaluated as indefinite, an arbitrary function of the variables ρ, ϕ and a must be added. However, it can be shown by considering the behavior at $z = \infty$ that this function is zero.

To evaluate the elastic field for shear loading, the relationship in eqn (D1) can be used along with the derivatives

$$\Delta\Phi(\rho,\phi,z) = \frac{i\pi}{2}(M\rho\,e^{-i\phi}-\bar{M}\rho\,e^{i\phi})\left\{\sin^{-1}\frac{\ell_1(a)}{\rho}+\frac{\ell_1(a)\sqrt{\rho^2-\ell_1^2(a)}}{\rho^2[\ell_2^2(a)-\ell_1^2(a)]}(a^2-\rho^2-z^2)\right\}, \tag{D3}$$

$$\Lambda^2\Phi(\rho,\phi,z) = \frac{i\pi}{2}M\,e^{i\phi}\left\{\rho\sin^{-1}\frac{\ell_1(a)}{\rho}+\frac{\ell_1(a)\sqrt{\rho^2-\ell_1^2(a)}}{\rho[\ell_2^2(a)-\ell_1^2(a)]}(a^2-\rho^2-z^2)\right\}+i\pi\bar{M}\,e^{3i\phi}\frac{\ell_1^3(a)[\rho^2-\ell_1^2(a)]^{3/2}}{\rho^3[\ell_2^2(a)-\ell_1^2(a)]}. \tag{D4}$$

The derivative $\Lambda^3\Phi(\rho,\phi,z)$ is in a more complicated form and it is not explicitly given here. It was pointed out in Appendix C that $\Lambda^3\psi(\rho,\phi,z)$ and $\Lambda^3\Phi(\rho,\phi,z)$ are not individually needed, only the combination $\Lambda^3(z\psi(\rho,\phi,z)-\Phi(\rho,\phi,z))$ is required. This combination has the simpler form given below as:

$$\Lambda^3(z\psi(\rho,\phi,z)-\Phi(\rho,\phi,z)) = i\pi M\,e^{i2\phi}\frac{\ell_1^3(a)\sqrt{\rho^2-\ell_1^2(a)}}{\rho^2[\ell_2^2(a)-\ell_1^2(a)]}$$
$$+i\pi\bar{M}\,e^{i4\phi}\left\{-\frac{8z}{\rho^4}(2a^3-[\ell_1^2(a)+2a^2]\sqrt{a^2-\ell_1^2(a)})\right.$$
$$\left.+\frac{6}{\rho^4}\ell_1^3(a)\sqrt{\rho^2-\ell_1^2(a)}-\frac{\ell_1^3(a)\sqrt{\rho^2-\ell_1^2(a)}}{\rho^2[\ell_2^2(a)-\ell_1^2(a)]}\right\}. \tag{D5}$$